

Supplementary materials for “An ultra-flexible plasmonic metamaterial film for efficient omnidirectional and broadband optical absorption”

HUI ZHANG,¹ LEI FENG,¹ YUZHANG LIANG,¹ AND TING XU^{1,*}

¹National Laboratory of Solid State Microstructures, College of Engineering and Applied Sciences and Collaborative Innovation Centre of Advanced Microstructures, Nanjing University, Nanjing 210093, China

*xuting@nju.edu.cn

1. Destruction of Kevlar Macro-Fibers

We performed Fourier transform infrared spectroscopy (FT-IR) tests on Kevlar macro-fiber and ANF films to characterize the destruction process, as shown in Figure S1. The intensity and sharpness of the peaks of the ANF IR spectra is less than that of the Kevlar macro-fiber due to the broader distribution of bond lengths and surface states of the fibers after the destruction. However, both two spectra are of an analogous profile because the chemical composition of Kevlar macro-fibers and ANFs are the same.

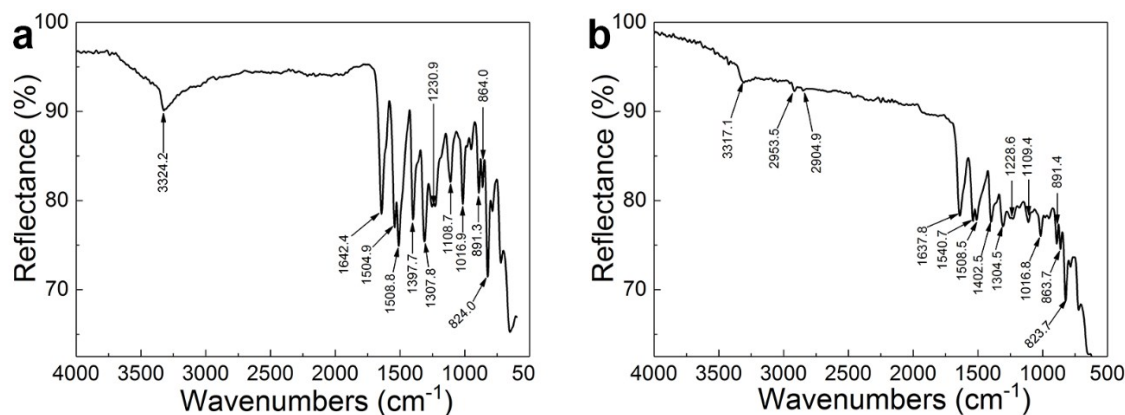


Fig. S1. FT-IR spectra comparing the (a) Kevlar macro-fiber and (b) the ANF films.

2. PMFs doped with different contents of Au NPs

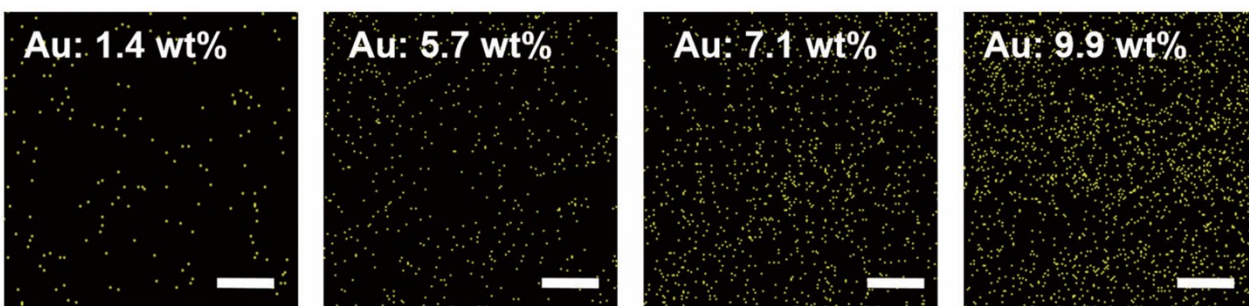


Fig. S2. Au elemental mapping of PMFs doped with 1.4 wt%, 5.7 wt%, 7.1 wt%, and 9.9 wt% Au NPs, respectively. The scale bars stand for 1 μm.

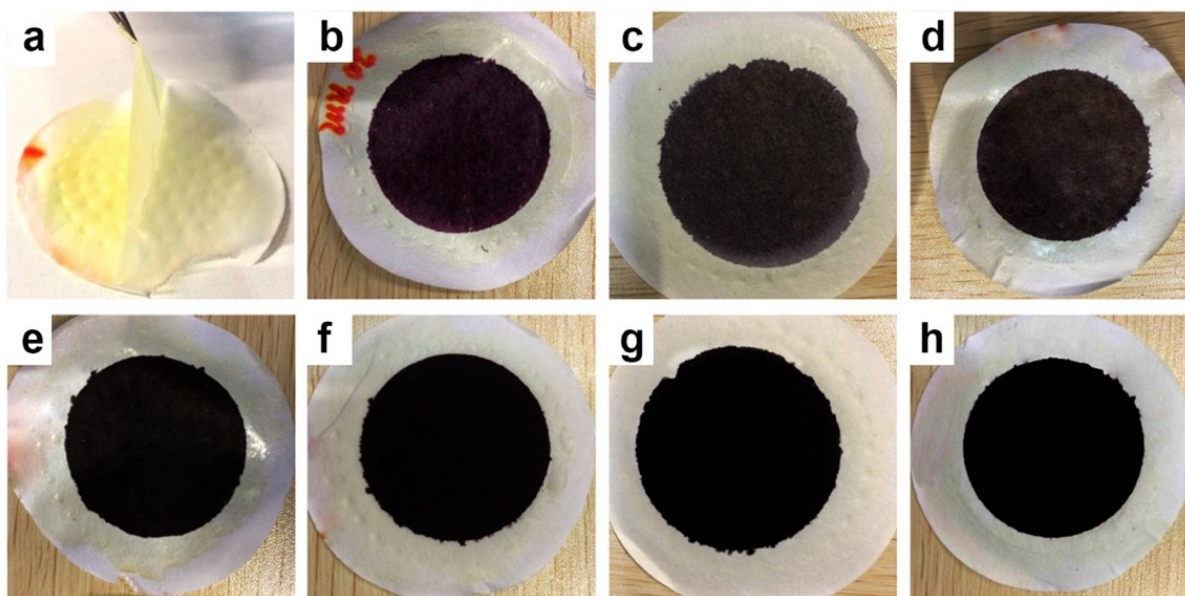


Fig. S3. (a)-(h) Photographs of Au-ANF PMFs with 0, 1.4%, 2.8%, 4.3%, 5.7%, 7.1%, 8.6% to 9.9% contents of Au NPs (diameter = 58 nm), respectively.

3. PMFs doped with Au NPs in different sizes

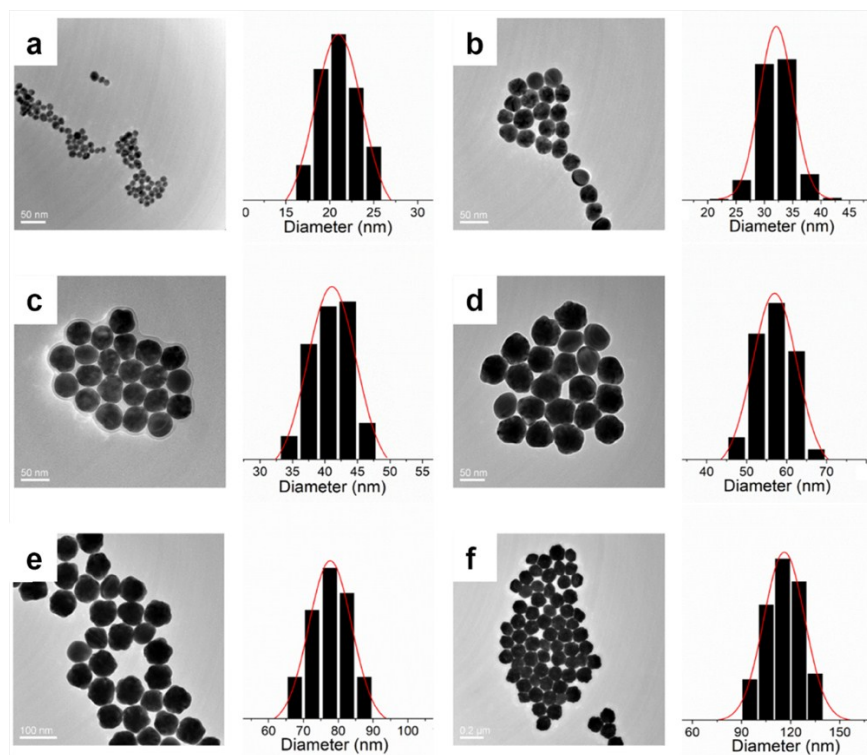


Fig. S4. (a)-(f) TEM characterizations of the Au NPs with 21 nm, 32 nm, 42 nm, 58 nm, 78 nm, and 115 nm diameters, respectively. (left) TEM image and (right) size distribution.

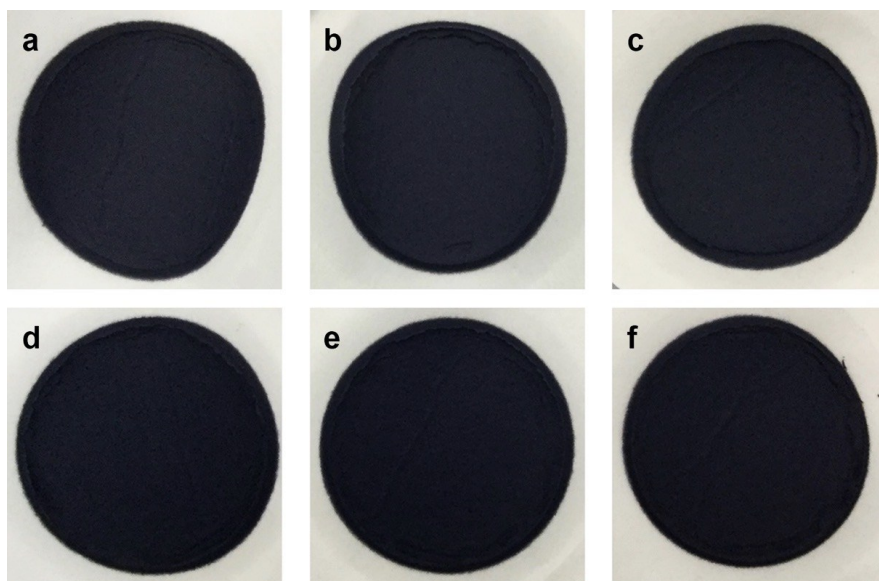


Fig. S5. (a)-(f) Photographs of PMFs doped with Au NPs (content = 5.7 wt %) of 21 nm, 32 nm, 42 nm, 58 nm, 78 nm and 115 nm diameters, respectively.

4. Numerical simulations

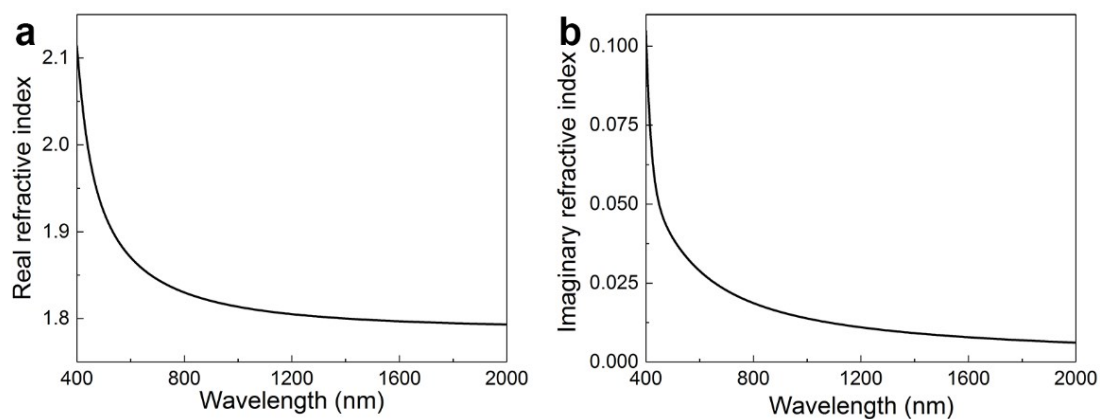


Fig. S6. Ellipsometry measured (a) real part and (b) imaginary part of the complex refractive index of ANF.

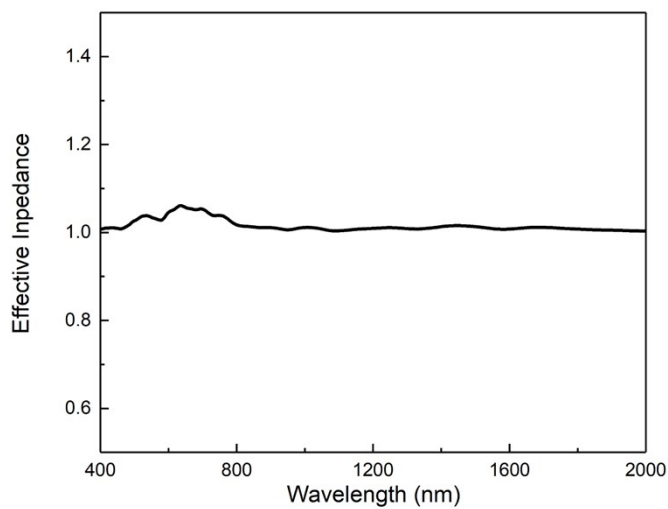


Fig. S7. Calculated effective impedance of the Au-ANF nanocomposite PMF.

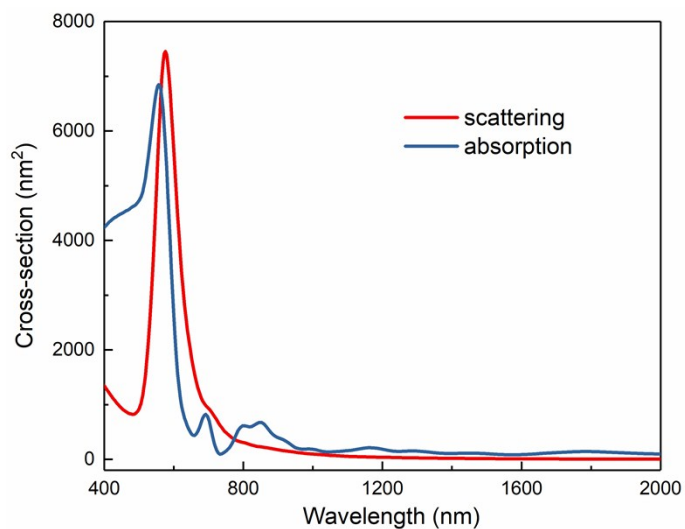


Fig. S8. Absorption and absorption cross-section of an isolated Au NP embedded in aramid.

5. Optical Property of the PMF after the bending test

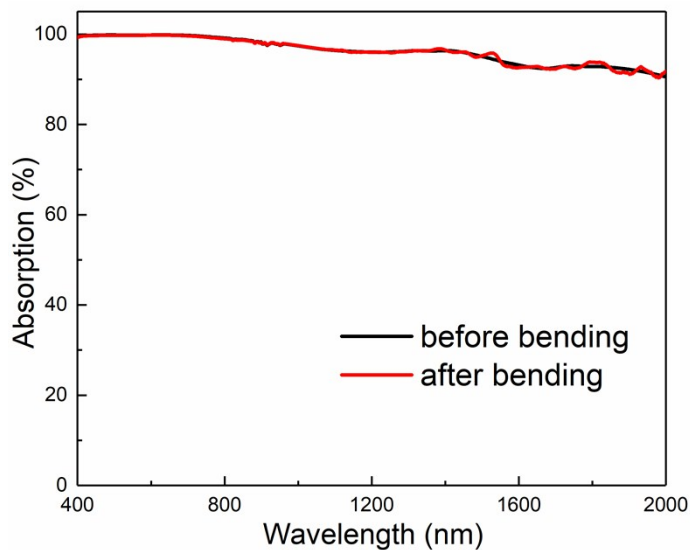


Fig. S9. Absorption spectra of the PMF before and after the bending test.